

Discovery of a Potent, Selective, and Orally Active Proteasome Inhibitor for the Treatment of Cancer

Bruce D. Dorsey,^{*,†} Mohamed Iqbal,[†] Sankar Chatterjee,[†] Ernesto Menta,[‡] Raffaella Bernardini,[‡] Alberto Bernareggi,[‡] Paolo G. Cassarà,[‡] Germano D'Arasmo,[‡] Edmondo Ferretti,[‡] Sergio De Munari,[‡] Ambrogio Oliva,[‡] Gabriella Pezzoni,[‡] Cecilia Allievi,[‡] Ivan Strepponi,[‡] Bruce Ruggeri,[†] Mark A. Ator,[†] Michael Williams,[†] and John P. Mallamo[†]

Cephalon, Inc., 145 Brandywine Parkway, West Chester, Pennsylvania 19380, and Cell Therapeutics Europe S.r.l., Via L. Ariosto, 23, I-20091 Bresso, Italy

Received August 27, 2007

The ubiquitin–proteasome pathway plays a central role in regulation of the production and destruction of cellular proteins. These pathways mediate proliferation and cell survival, particularly in malignant cells. The successful development of the 20S human proteasome inhibitor bortezomib for the treatment of relapsed and refractory multiple myeloma has established this targeted intervention as an effective therapeutic strategy. Herein, the potent, selective, and orally bioavailable threonine-derived 20S human proteasome inhibitor that has been advanced to preclinical development, [(1*R*)-1-[[[(2*S*,3*R*)-3-hydroxy-2-[(6-phenylpyridine-2-carbonyl)amino]-1-oxobutyl]amino]-3-methylbutyl]boronic acid **20** (CEP-18770), is disclosed.

Introduction

The ubiquitin–proteasome pathway (UPP) is responsible for most intracellular degradation of proteins in eukaryotes. Within the cytosol and nucleus, ubiquitin is activated by an ubiquitin-activating enzyme (E1) and transferred to an ubiquitin-conjugating enzyme (E2). Specific binding of E2 enzyme with substrate–protein to an ubiquitin–protein ligase (E3) permits the transfer of a polyubiquitin chain. Once tagged, these polyubiquitin proteins are then degraded by 26S proteasome into ubiquitin and short peptides that are further processed into recyclable amino acids.^{1,2} The proteolytic component of the UPP consists of a multicatalytic protein core particle (CP) known as the 20S proteasome capped by two 19S regulatory particles (RPs). The RPs are responsible for recognition, unfolding, and translocation of protein–substrates into the CP cavity where proteolytic processing occurs. Crystal structures of eukaryotic 20S proteasomes reveal an elongated shaped cylinder for the CP, which contains four stacked rings. Each ring is composed of seven different α and β subunits where the outer α rings of the complex interact with the RPs and the two inner β rings contain the proteolytically active sites.³ Three different active sites are responsible for the postglutamyl (β 1), tryptic (β 2), and chymotryptic (β 5) proteolytic activities.⁴ Each utilizes the nucleophilic γ -hydroxyl group of the N-terminal threonine (Thr) to initiate amide bond hydrolysis followed by activation of nucleophilic water by the α -amine of Thr to hydrolyze the resulting ester.

Among the various enzymatic activities of the proteasome, the “chymotrypsin-like” activity has emerged as the biological function of greatest interest and focus of drug discovery efforts. Increased levels of this enzyme and subsequent protein breakdown have been implicated in many disease states including muscular dystrophy, emphysema, cancers such as acute myeloid leukemia, and cachexia accompanying cancer and AIDS.⁵ Proteasome function also controls levels of proteins critical for cell cycle control, including p53, p27, and cyclin B and is

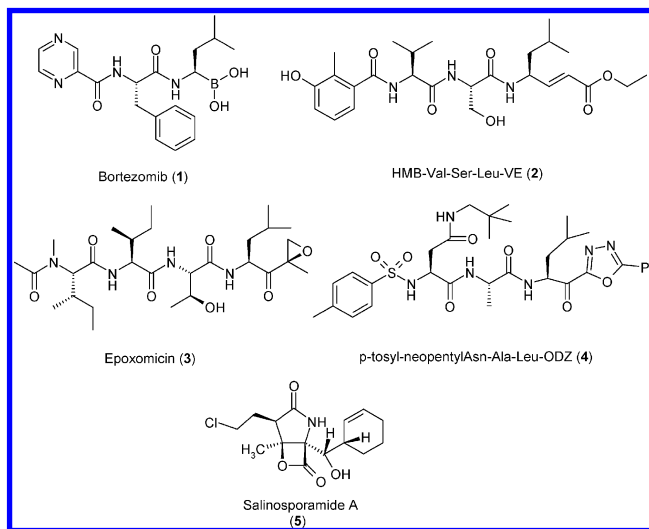


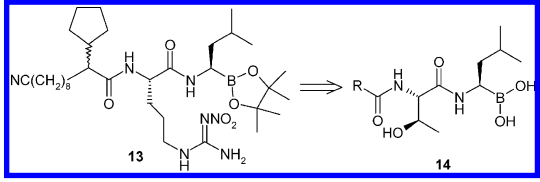
Figure 1. Structures of bortezomib, vinyl ester tripeptides, epoxomicin, reversible 2-keto-1,3,4-oxadiazoles, and the natural product salinosporamide A.

responsible for activation of the transcription factor NF- κ B through the degradation of its regulatory subunit I κ B α .⁶ Thus, development of proteasome inhibitors has emerged as an attractive target for cancer therapy.^{7,8} Clinical validation of this approach has been demonstrated with bortezomib **1** (Figure 1), a proteasome inhibitor recently approved as a single agent for the treatment of patients with relapsed and refractory multiple myeloma with at least one prior line of therapy and for the treatment of mantle cell lymphoma.^{9,10} Although this drug has demonstrated higher overall response rates and prolonged survival compared to standard treatments, such as dexamethasone, some liabilities exist. Bortezomib is administered as an intravenous bolus, and dose-limiting toxicities, adverse events, and resistance to single agent therapy have been reported.¹¹ Therefore, there remains a significant need to develop new proteasome inhibitors with potentially unique properties, including activity following oral administration, different proteasome inhibition profile, and greater therapeutic index.

* To whom correspondence should be addressed. Phone: (610) 738-6472. Fax: (610) 738-6643. E-mail: bdorsey@cephalon.com.

[†] Cephalon, Inc.

[‡] Cell Therapeutics Europe S.r.l.

Table 1. Proteasome Inhibitory Activity


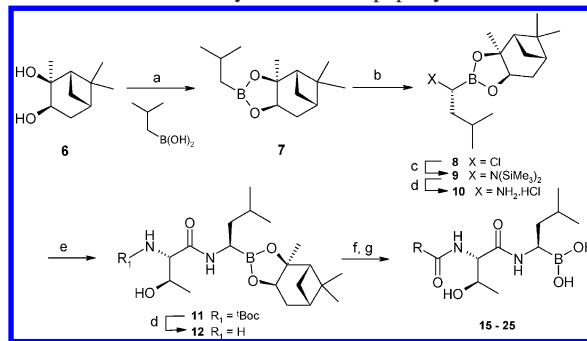
compd	R	HEP IC ₅₀ (SD), nM	CHY IC ₅₀ (range μ M), μ M	Molt-4 EC ₅₀ (SD), nM	A2780 IC ₅₀ (SD), nM
15	pyrazin-2-yl	42.0 (2.1)	ND	1353 (19.2)	ND
16	naphthalen-2-yl	1.6 (0.1)	0.5 (0.3–0.8)	27 (6)	5.3 (3.1)
17	quinolin-2-yl	6.8 (0.4)	1.30 (1.0–1.8)	32 (8.5)	20.9 (7.5)
18	4-biphenyl	0.9 (0.2)	0.6 (0.3–0.9)	21 (1.4)	4.9 (1.2)
19	3-biphenyl	0.8 (0.1)	0.9 (0.8–1.0)	16.9 (5.4)	4.8 (4.0)
20	6-phenylpyridin-2-yl	3.8 (1.0)	1.5 (0.9–1.8)	13.5 (2.0)	13.7 (2.3)
21	4-phenylpyridin-2-yl	2.0 (0.1)	0.29 (0.2–0.4)	18.6 (1.0)	5.1 (2.7)
22	3-phenyl-pyridin-2-yl	8.8 (1.1)	0.46 (0.3–0.6)	13000 (100)	ND
23	5-phenylpyrazin-2-yl	1.8 (0.1)	0.27 (0.2–0.4)	21 (5.0)	8.2 (2.9)
24	6-phenylpyrazin-2-yl	2.3 (0.2)	0.28 (0.3–0.5)	27 (6.0)	9.8 (2.9)
25	2-phenyl-thiazol-4-yl	4.6 (0.4)	0.59 (0.5–0.61)	16 (3.0)	28.0 (3.8)
1	bortezomib	3.8 (0.4)	0.5 (0.3–0.9)	21 (3.0)	1.7 (0.4)

Several years ago, starting from a tetrapeptide aldehyde inhibitor, novel, potent, and selective dipeptide aldehyde inhibitors of the chymotrypsin-like activity of the proteasome were identified.¹² Subsequently, **12** (Table 1) and related analogues emerged as a useful tools in proteasome research.¹³ Other research groups have disclosed reversible and irreversible peptide-based inhibitors of the 20S proteasome. The vinyl ester inhibitor **2** (Figure 1) represents a series of irreversible inhibitors¹⁴ with submicromolar trypsin-like activity and limited chymotrypsin-like activity. Conversely, Crews et al.¹⁵ reported irreversible epoxomicin analogues (**3**) with β 1 and β 5 selectivity that demonstrate the independent nature of the active site functions. Potent, selective, and reversible inhibitors of the chymotrypsin-like activity possessing a unique keto-1,3,4-oxadiazole warhead have been reported by Rydzewski.¹⁶ Represented by **4**, this subnanomolar inhibitor is active against the proteasome contained in PC3 cells, a human prostate cancer cell line. A recently discovered natural product, salinosporamide A (**5**) from the marine microorganism *Salinispora tropica*, has been reported that displays nanomolar potency against the 20S proteasome¹⁷ and oral antitumor activity in xenograft model studies.¹⁸

In our continued search for a potent and druglike proteasome inhibitor, additional boronate-derived small-molecule inhibitors were explored. Building on previous advances, potent boronic esters were identified. Ultimately, this led to identification of an orally active proteasome inhibitor that is currently being evaluated for development opportunities.

Results and Discussion

Synthesis. The generalized preparation of dipeptidyl boronic acids, specifically (2*S*,3*R*)-2-amino-3-hydroxybutyric acids represented by **14**, is illustrated in Scheme 1. Following a procedure of Matteson,¹⁹ benzodioxaborole **8** was obtained in 92% yield over two steps and in high enantiomeric purity from commercially available starting materials. Treatment of benzodioxaborole **8** with lithium bis(trimethylsilyl)amide produced protected amine **9** that underwent facile deprotection in HCl to generate the desired amino boronate **10** as the hydrochloride salt in 66% overall yield on a 50 g scale.²⁰ Amino boronate **10** was coupled with *t*-Boc-L-threonine to provide, after chromatographic purification, amide **11** which was deprotected with hydrochloric acid in dioxane to produce the versatile intermediate **12** in 50% yield. Only one diastereomer was detected by

Scheme 1. Generalized Synthesis of Dipeptidylboronic Acids^a

^a Reagents and conditions: (a) Et₂O, room temp, 24 h; (b) (i) CH₂Cl₂, THF, LDA, –78°C; (ii) 1.0 M ZnCl₂ in ether, –78°C; (c) LiN(SiMe₃)₂, THF, –78 °C to room temp; (d) HCl in dioxane, ether, 0°C; (e) *t*-Boc-L-threonine, NMM, TBTU, DMF, 0°C; (f) RCOOH, TBTU, NMM, DMF, 0°C; (g) isobutylboronic acid, 2 N HCl, MeOH, hexane.

¹H NMR. Coupling of amine **12** to various acids followed by acid catalyzed ester exchange with isobutylboronic acid provided target compounds **13–25** (44–75% yield for two steps).

Biological Results. Proteasome inhibitory activity of the target compounds was evaluated in an isolated 20S human erythrocyte proteasome (HEP) fluorimetric kinetic assay of chymotrypsin-like proteasome activity.¹² Activity of the compounds was also investigated in the human leukemia cell line Molt-4 using the fluorogenic chymotrypsin-like cell permeable fluorogenic substrate MeOSuc-FLF-AFC, following a published procedure; thus, this assay also served as a measure of cell permeability of an inhibitor.¹³ Determination of cross-reactivity against human pancreas α -chymotrypsin (CHY) using a fluorogenic specific substrate was also assessed. Table 1 displays the biological data, expressed as IC₅₀ values for HEP and CHY assays, and EC₅₀ values for Molt-4. The antiproliferative activity was determined in A2780 ovarian carcinoma cell line using standard colorimetric assay to assess cell proliferation and cellular viability. Additional selectivity data were obtained against a panel of proteases representing all mechanistic classes of proteases (see Supporting Information, Table S1).

Discussion

As summarized in Table 1, initial attempts to identify a superior small-molecule proteasome inhibitor involved modification of the previously reported boronic ester **13**.¹² Amino

acid scanning of the P2 position, including phenylalanine, glycine, 2,3-diaminopropionic acid, citrulline, and asparagine, resulted in the replacement of the nitroarginine moiety in **13** with threonine. Subsequent exploration of the P3 position with small, focused libraries revealed that replacement of branched alkyl moieties with naphthyl, quinolyl, or biaryl ligands provided the required potency and elimination of a chiral center. All compounds inhibited the chymotrypsin-like activity of 20S proteasome with IC₅₀ values from 0.8 to 42 nM. Initially, to benchmark our efforts against bortezomib,²¹ the pyrazine **15**, in which the P2 ligand threonine replaced phenylalanine, was prepared. Despite the structural similarity, this resulted in an 11-fold loss in enzyme potency and greater than 50-fold loss in cellular activity for **15** versus **1**. This result focused our efforts on substituted phenyl rings and heterocyclic biaryl moieties. The fused bicyclic aryls (i.e., **16** or **17**) or the 4- or 3-substituted biphenyl (**18**, **19**) analogues exhibited excellent enzyme, cellular, and antiproliferation activities. Of note, the 3-biphenyl **19** inhibited pancreatic α -chymotrypsin with IC₅₀ = 900 nM, demonstrating a greater than 1000-fold selectivity for the 20S proteasome versus bovine α -chymotrypsin activity. This selectivity trend continued with the 6- and 4-phenyl substituted pyridylcarboxamide analogues **20**²² and **21**, respectively. Erosion of this selectivity was observed for the 3-phenyl substituted pyridine **22**. This phenyl substituted regioisomer has HEP IC₅₀ = 8.8 nM and CHY IC₅₀ = 460 nM with only 52-fold selectivity for the 20S proteasome. A loss in cellular potency was observed (Molt-4 EC₅₀ = 13 000 nM), and further ortho substituted analogues were not pursued. Modifications of the P3 ligand with phenyl substituted pyrazines (**23**, **24**) or 2-phenyl-4-thiazole-carboxamide **25** provided molecules with comparable enzyme and cellular potency but with somewhat diminished selectivity versus α -chymotrypsin.

The selectivity of pyridyl analogue **20** and bortezomib was assessed in a broad panel of 42 protease assays, representing all protease mechanistic classes. While most serine proteases were not affected, modest inhibition of cathepsin G, chymase, and chymotrypsin was observed for both compounds (Supporting Information, Table S1), with IC₅₀ values 150- to 1500-fold greater than their proteasome chymotrypsin-like inhibitory activities. Some inhibition of neutrophil elastase 2 was also detected for **20**. No inhibition of cysteine proteases or the mechanistically distinct metalloproteases and aspartyl proteases was observed.

To further probe the role proteasome plays in cell viability and proliferation, the cytotoxic effects of the compounds on cell growth of a human ovarian CA solid tumor A2780 were accessed. Importantly, two of the most active compounds in the Molt-4 cellular assay, 3-biphenyl **19** (EC₅₀ = 16.9 nM) and pyridyl **20** (EC₅₀ = 13.5 nM), were also potent in an antiproliferation assay with IC₅₀ of 4.8 and 13.7 nM, respectively. The 4-fold loss of potency from enzyme to cell for **20** is minimal, demonstrating excellent cell membrane permeation for this analogue.

These compounds were further differentiated by profiling several for iv and oral pharmacokinetics in female Sprague–Dawley rats and CD-1 mice. Of the compounds described in Table 1, **20** demonstrated superior pharmacokinetic parameters, and a comparison with bortezomib is illustrated in Table 2.

When dosed in female Sprague–Dawley rats, **20** was slowly eliminated with estimated terminal half-lives of 71 and 86 h after iv and oral administration, respectively, and 15 and 53 h, respectively, in CD-1 mice (Table 2). This long elimination

Table 2. Single Dose iv and po Pharmacokinetic Profiles of **20** and **1** in Rats and Mice

compd	species	dose (mg/kg)	t _{1/2} (h)	AUC _{0–∞} (ng·h/mL)	V _{ss} (L/kg)	CL ((L/h)/kg)	F (%)
20	S-D rat	0.2 iv	71	1030	18.1	0.19	54
		0.8 po	86	2200			
	CD-1 mice	4 iv	15	2910	10.3	1.4	39
		10 po	53	2850			
1	CD-1 mice	0.8 iv	98	927	102	0.86	11
		4 po	70	499			

phase half-life is due in part to the large volume of distribution, V_{ss} = 18.1 L/kg in rats and 10.3 L/kg in mice, and very low systemic clearance in rats and mice (0.19 and 1.4 (L/h)/kg, respectively). This experimental observation is consistent with the lipophilicity, protein binding, and in vitro metabolic stability in rat and murine liver microsomes (see Supporting Information Tables S2 and S3). The absolute oral bioavailabilities of **20** in rats and mice were 54% and 39%, respectively. The bioavailability and systemic clearance data in relation to hepatic blood flow in rodents suggest that limited first pass metabolism of **20** and bortezomib occurs in the liver. The lower oral bioavailability of bortezomib is possibly due to reduced absorption in the mouse gastrointestinal tract. Previous studies have shown that bortezomib is orally bioactive^{23,24} in models of antigen-induced arthritis and lung carcinoma xenografts. However, the current bortezomib therapy in multiple myeloma is administered intravenously. Another proteasome inhibitor, **5**, has recently been reported to demonstrate comparable activity to bortezomib in a human subcutaneous plasmacytoma xenograft model after oral dosing.¹⁸ The pharmacokinetic profiles for **20** and bortezomib in rodents were characterized by prolonged exposure in the systemic circulation with a long terminal phase half-life, low systemic clearance, and a large volume of distribution. Despite the similarity in biochemical proteasome inhibition and subunit binding kinetics of **20** and bortezomib in normal and tumor cell lysates, **20** at its iv maximum tolerated dose (MTD) in mice demonstrated 86% inhibition of proteasome β 5/ β 1 subunit binding in subcutaneous human RPMI 8226 xenograft tissues in vivo in contrast to that observed with bortezomib (48% maximum inhibition of β 5/ β 1 subunit binding) at its corresponding i.v. MTD in mice.²⁵ Also, **20** and bortezomib showed comparable potency against chymotrypsin-like proteasome activity but demonstrated marginal inhibition of the tryptic and peptidyl glutamyl activities of the proteasome.

To further profile the in vitro characteristics of **20**, the in vitro microsomal metabolic stability, protein binding, and cytochrome P-450 inhibition were assessed in comparison to bortezomib. Stability in microsomes was measured, and this provided an indication of potential phase I oxidative metabolism (see Supporting Information, Table 2S). An assessment of cytochrome P-450 enzyme inhibition, indicative of potential drug–drug interactions, was also conducted using recombinant human P-450 enzymes and fluorescent P-450 substrates. Inhibition of the major P-450 isoforms 1A2, 2C9, 2C19, and 2D6 at concentrations up to 30 μ M was not observed; however, **20** and bortezomib did inhibit 3A4 (IC₅₀ of 3.5 and 17 μ M, respectively). Determination of plasma protein binding by ultracentrifugation, analyzed by high-throughput liquid chromatography coupled to a mass spectrometer (see Supporting Information, Table 3S) revealed that both inhibitors were protein bound across species. However, the free fraction of **20** was significantly lower than bortezomib in the presence of human serum albumin. These data suggest that higher plasma exposure of compound **20** may

be required in patients to achieve a comparable therapeutic benefit to bortezomib.

Conclusion

In this work, (2*S*,3*R*)-2-amino-3-hydroxybutyric acid derivatives designed and synthesized as inhibitors of the 20S human erythrocyte proteasome are disclosed. Prototypes of these dipeptylboronic acids were potent and selective for chymotrypsin-like proteasome activity and were cell-permeable. Analogue **20** was one of the more active and selective of these inhibitors and was also orally bioavailable in rodents. This compound has demonstrated in vivo efficacy versus bortezomib in several systemic human multiple myeloma xenograft models and a similar to superior toxicity profile in mice and rats.²⁵ An orally administered treatment for patients with relapsed and refractory multiple myeloma could represent a significant advance in the field of proteasome inhibitor therapy in oncology. On the basis of its in vitro potency, in vivo anticancer activities (rodent), and druglike properties, **20** has been selected for additional preclinical profiling for multiple myeloma therapy.

Experimental Section

Carbamic Acid 1,1-Dimethylethyl Ester, *N*-[(1*S*,2*R*)-1-[[[(1*R*)-1-[(3*aS*,4*S*,6*S*,7*aR*)-Hexahydro-3*a*,5,5-trimethyl-4,6-methano-1,3,2-benzodioxaborol-2-yl]-3-methylbutyl]amino]carbonyl]-2-hydroxypropyl] (11). To a cooled solution (0 °C) of Boc-L-threonine (9.6 g, 43.76 mmol) dissolved in anhydrous DMF (60 mL) was added TBTU (14.06 g, 43.76 mmol), NMM (13.2 mL, 120 mmol), and the known **10** (12 g, 39.8 mmol). The mixture stirred at room temperature for 16 h, poured into water, and extracted with EtOAc (3 × 200 mL). Combined organics were washed with 2% citric acid, 2% NaHCO₃, and brine, dried over anhydrous MgSO₄, filtered, and evaporated to provide crude product. Chromatography on silica gel using EtOAc/hexane gradient (from 20% to 75%) afforded 13.1 g (71%) of **11** as a glassy solid: mp 25°–30 °C; ¹H NMR (DMSO-*d*₆) δ 8.88 (br, 1H), 6.49 (d, *J* = 8.4 Hz, 1H), 4.88 (d, *J* = 5.8 Hz, 1H), 4.05 (m, 1H), 3.93 (m, 1H), 2.89 (m, 1H), 2.51 (m, 1H), 2.19 (m, 1H), 2.01 (m, 1H), 1.83 (t, *J* = 5.9 Hz, 1H), 1.78 (m, 1H), 1.68 (m, 1H), 1.62 (m, 1H), 1.39 (s, 9H), 1.34 (d, *J* = 10.0 Hz, 1H), 1.24 (s, 3H), 1.22 (s, 3H), 1.06 (d, *J* = 6.4 Hz, 3H), 0.85 (d, *J* = 6.4 Hz, 6H), 0.80 (s, 3H).

(2*S*,3*R*)-2-Amino-3-hydroxybutanamide, *N*-[(1*R*)-1-[(3*aS*,4*S*,6*S*,7*aR*)-Hexahydro-3*a*,5,5-trimethyl-4,6-methano-1,3,2-benzodioxaborol-2-yl]-3-methylbutyl]-, Hydrochloride Salt (12). To a solution of **11** (13.1 g, 28.1 mmol) dissolved in anhydrous diethyl ether (40 mL) at 0 °C was added 2 N HCl in diethyl ether (98 mL, 196 mmol). The mixture was stirred overnight and slowly allowed to warm to room temperature. The resulting white solid was collected by filtration, washed, and dried under vacuum to afford 7.9 g (70% yield) of **12** as a white solid. A second, less pure crop was obtained from the mother liquors by concentration to dryness (3.0 g, 26% yield). ¹H NMR (DMSO-*d*₆) δ 8.62 (d, *J* = 5.0 Hz, 1H), 8.17 (d, *J* = 3.5 Hz, 3H), 4.28 (dd, *J* = 8.8, 1.8 Hz, 1H), 3.78 (m, 1H), 3.52 (m, 1H), 3.00 (m, 1H), 2.28 (m, 1H), 2.10 (m, 1H), 1.92 (t, *J* = 5.7 Hz, 1H), 1.84 (m, 1H), 1.75–1.62 (m, 2H), 1.43 (m, 1H), 1.31 (s, 3H), 1.25 (s, 3H), 1.22 (d, *J* = 10.6 Hz, 1H), 1.14 (d, *J* = 6.2 Hz, 3H), 0.88 (d, *J* = 6.4 Hz, 3H), 0.86 (d, *J* = 6.4 Hz, 3H), 0.81 (s, 3H).

***N*-[(1*S*,2*R*)-1-[[[(1*R*)-1-[(3*aS*,4*S*,6*S*,7*aR*)-Hexahydro-3*a*,5,5-trimethyl-4,6-methano-1,3,2-benzodioxaborol-2-yl]-3-methylbutyl]amino]carbonyl]-2-hydroxypropyl]-6-phenyl-2-pyridine-carboxamide.** To a solution of commercially available 6-phenylpyridine-2-carboxylic acid (220 mg, 1.10 mmol) dissolved in DMF (15 mL) and cooled to 0 °C were added TBTU (400 mg, 1.2 mmol), NMM (0.35 mL, 3.2 mmol), and **12** (430 mg, 1.067 mmol). The mixture was stirred for 2 h, poured in water, and extracted with EtOAc. The combined organic layer was washed with 2% citric acid, 2% NaHCO₃, and brine, dried over MgSO₄, filtered, and

concentrated to provide crude oil. Flash column chromatography on silica gel using EtOAc/hexane gradient (30%) afforded 257 mg (44%) of product as a white solid. ¹H NMR (DMSO-*d*₆, 400 MHz) δ 8.98 (d, *J* = 2.99 Hz, 1H), 8.76 (d, *J* = 8.55 Hz, 1H), 8.2 (m, 3H), 8.11 (t, *J* = 7.71 Hz, 1H), 8.02 (d, *J* = 7.54 Hz, 1H), 7.54 (m, 3H), 5.26 (d, *J* = 4.95 Hz, 1H), 4.49 (dd, *J* = 8.52, 4.22 Hz, 1H), 4.13 (m, 2H), 2.6 (m, 1H), 2.19 (m, 1H), 2.02 (m, 1H), 1.83 (t, *J* = 5.38 Hz, 1H), 1.75 (s, 1H), 1.68 (m, b, 1H), 1.62 (d, *J* = 13.9 Hz, 1H), 1.36 (d, *J* = 10.05 Hz, 1H), 1.3 (m, b, 3H), 1.22 (d, *J* = 11.65 Hz, 6H), 1.12 (d, *J* = 6.26 Hz, 3H), 0.84 (d, *J* = 6.57 Hz, 6H), 0.79 (s, 3H).

[(1*R*)-1-[(2*S*,3*R*)-3-Hydroxy-2-[(6-phenylpyridine-2-carboxyl)amino]-1-oxobutyl]amino]-3-methylbutyl]boronic Acid (20). A solution of *N*-[(1*S*,2*R*)-1-[[[(1*R*)-1-[(3*aS*,4*S*,6*S*,7*aR*)-hexahydro-3*a*,5,5-trimethyl-4,6-methano-1,3,2-benzodioxaborol-2-yl]-3-methylbutyl]amino]carbonyl]-2-hydroxypropyl]-6-phenyl-2-pyridinecarboxamide (240 mg, 0.438 mmol), 2-methylpropylboronic acid (112 mg, 1.095 mmol), and 2 N aqueous HCl (0.44 mL) in a heterogeneous mixture of methanol (3 mL) and hexane (3 mL) was stirred at room temperature for 16 h. The methanolic layer was removed, and the hexane layer was extracted with methanol (5 mL). The combined methanolic layers were combined and concentrated, and the resulting residue was dissolved in EtOAc (30 mL). This was washed with 8% aqueous NaHCO₃, and the basic layers were combined and extracted with EtOAc. The combined organic phases were dried over sodium sulfate, concentrated in vacuo, and chromatographed on silica gel using EtOAc/hexane gradient (50%) followed by increasing amounts of methanol to elute 94 mg (52%) of **20** as an off-white solid. HPLC indicates a purity of 97.6 area %. ¹H NMR (CD₃OD, 400 MHz) δ 8.17 (m, 2H), 8.13 (m, 1H), 8.05 (m, 2H), 7.5 (m, 3H), 4.75 (d, *J* = 3.04 Hz, 1H), 4.42 (dq, *J* = 6.4, 2.92 Hz, 1H), 2.77 (t, b, 1H), 1.61 (m, 1H), 1.35 (t, *J* = 7.48 Hz, 2H), 1.29 (d, *J* = 6.36 Hz, 3H), 0.89 (d, *J* = 6.52 Hz, 6H); ¹³C NMR (CD₃OD) δ 20.76, 22.64, 23.78, 27.17, 41.14, 57.19, 68.13, 121.93, 124.95, 128.16, 130.04, 131.18, 139.48, 140.24, 150.05, 157.79, 167.23, 177.43; MS *m/z* 452 (M + K), 436 (M + Na), 396 (M – OH), 378, 352, 264. HRMS (M + Na) Calcd: 435.2056. Found: 435.2057. Anal. Calcd for C₂₁H₂₈BN₃O₅: C, 61.03; H, 6.83; N, 10.17%. Found: C, 63.22; H, 6.52; N, 10.17%.

Acknowledgment. We thank Drs. Jeffery Vaught and James C. Kauer for their support and encouragement and acknowledge the efforts of Dr. Renee Roemmele and Process Chemistry for the large scale preparation of **20**.

Note Added after Print Publication. To correct a printing error related to Scheme 1, this paper was reposted on March 14, 2008.

Supporting Information Available: ¹H NMR, HRMS, and elemental analysis results for **7–10**, **15–19**, and **21–25** and details of biological assay conditions. This material is available free of charge via the Internet at <http://pubs.acs.org>.

References

- (1) Ciechanover, A. Intracellular protein degradation: from a vague idea, through the lysosome and the ubiquitin–proteasome system, and onto human diseases and drug targeting (Nobel lecture). *Angew. Chem., Int. Ed.* **2005**, *44*, 5944–5967.
- (2) Goldberg, A. L. Functions of the proteasome: from protein degradation and immune surveillance to cancer therapy. *Biochem. Soc. Trans.* **2007**, *35*, 12–17.
- (3) Groll, M.; Ditzel, L.; Lowe, J.; Bochtler, M.; Bartunik, H.; Huber, R. Structure of 20S proteasome from yeast at 2.4 Å resolution. *Nature* **1997**, *386*, 463–471.
- (4) Groll, M.; Heinemyer, W.; Jager, S.; Ullrich, T.; Bochtler, M.; Wolf, D. H.; Huber, R. The catalytic sites of 20S proteasomes and their role in subunit maturation: a mutational and crystallographic study. *Proc. Natl. Acad. Sci. U.S.A.* **1999**, *96*, 10976–10983.
- (5) Delcros, J. G.; Baudy Floch, M.; Prigent, C.; Arlot-Bonnemains, Y. Proteasome inhibitors as therapeutic agents: current and future strategies. *Curr. Med. Chem.* **2003**, *10*, 479–503.
- (6) Rolfe, M.; Chiu, M. I.; Pagano, M. The ubiquitin-mediated proteolytic pathway as a therapeutic area. *J. Mol. Med.* **1997**, *75*, 5–17.

- (7) Mitsiades, C. S.; Mitsiades, N.; Hideshima, T.; Richardson, P. G.; Anderson, K. C. Proteasome inhibition as a new therapeutic principle in hematological malignancies. *Curr. Drug. Targets* **2006**, *7*, 1341–1347.
- (8) Rajkumar, S. V.; Richardson, P. G.; Hideshima, T.; Anderson, K. C. Proteasome inhibition as a novel therapeutic target in human cancer. *J. Clin. Oncol.* **2005**, *23*, 630–639.
- (9) (a) Bortezomib is marketed as Velcade by Millennium Pharmaceuticals, Inc., of Cambridge, MA. (b) Adams, J. The development of proteasome inhibitors as anticancer drugs. *Cancer Cell* **2003**, *5*, 417–412.
- (10) Orlowski, R. Z.; Zeger, E. L. Targeting the proteasome as a therapeutic strategy against hematological malignancies. *Expert Opin. Invest. Drugs* **2006**, *15*, 117–130.
- (11) Richardson, P. G.; Sonneveld, P.; Schuster, M. W.; Irwin, D.; Stadtmauer, E. A.; Facon, T.; Harousseau, J.-L.; Ben-Yehuda, D.; Lonial, S.; Goldschmidt, H.; Reece, D.; San-Miguel, J. F.; Blade, J.; Boccadoro, M.; Cavenaugh, J.; Dalton, W. S.; Boral, A. L.; Esseltine, D. L.; Porter, J. B.; Schenkein, D.; Anderson, K. C. Bortezomib or high-dose dexamethasone for relapsed multiple myeloma. *N. Engl. J. Med.* **2005**, *352*, 2487–2498.
- (12) (a) Iqbal, M.; Chatterjee, S.; Kauer, J. C.; Das, M.; Messina, P.; Freed, B.; Biazio, W.; Siman, R. Potent inhibitors of the proteasome. *J. Med. Chem.* **1995**, *38*, 2276–2277. (b) Iqbal, M.; Chatterjee, S.; Kauer, J. C.; Mallamo, J. P.; Messina, P. A.; Reiboldt, A.; Siman, R. Potent α -ketocarbonyl and boronic ester-derived inhibitors of the proteasome. *Bioorg. Med. Chem. Lett.* **1996**, *6*, 287–290.
- (13) Sun, J.; Nam, S.; Lee, C.; Li, B.; Coppola, D.; Hamilton, A. D.; Dou, Q. P.; Sebt, S. M. CEP1612, a dipeptidyl proteasome inhibitor, induces p21^{WAF1} and p27^{KIP1} expression and apoptosis and inhibits the growth of the human A-549 in nude mice. *Cancer Res.* **2001**, *61*, 1280–1284.
- (14) Marastoni, M.; Baldisserotto, A.; Cellini, S.; Gavioli, R.; Tomatis, R. Peptidyl vinyl ester derivatives: new class of selective inhibitors of the proteasome trypsin-like activity. *J. Med. Chem.* **2005**, *48*, 5038–5042.
- (15) Meng, L.; Mohan, R.; Kwok, B.; Eloffsson, M.; Sin, N.; Crews, C. Epoxomicin, a potent and selective proteasome inhibitor, exhibits in vivo anti-inflammatory activity. *Proc. Natl. Acad. Sci. U.S.A.* **1999**, *96*, 10403–10408.
- (16) Rydzewski, R. M.; Burrill, L.; Mendonca, R.; Palmer, J. T.; Rice, M.; Tahiramani, R.; Bass, K. E.; Leung, L.; Gjerstad, E.; Janc, J. W.; Pan, L. Optimization of subsite binding to the b5 subunit of the human 20S proteasome using vinyl sulfones and 2-keto-1,3,4-oxadiazoles: synthesis and cellular properties of potent, selective, proteasome inhibitors. *J. Med. Chem.* **2006**, *49*, 2953–2968.
- (17) Feling, R. H.; Buchanan, G. O.; Mincer, T. J.; Kauffman, C. A.; Jensen, P. R.; Fenical, W. F. Salinosporamide A: a highly cytotoxic proteasome inhibitor from a novel microbial source, a marine bacterium of the new genus *Salinospora*. *Angew. Chem., Int. Ed.* **2003**, *42*, 355–357.
- (18) Chauhan, D.; Catley, L.; Li, G.; Podar, K.; Hideshima, T.; Velankar, M.; Mitsiades, C.; Mitsiades, N.; Yasui, H.; Letai, A.; Ovaa, H.; Berkers, C.; Nicholson, B.; Chao, T.-H.; Neuteboom, S. T. C.; Richardson, P.; Palladino, M. A.; Anderson, K. C. A novel orally active proteasome inhibitor induces apoptosis in multiple myeloma cells with mechanisms distinct from bortezomib. *Cancer Cell* **2005**, *8*, 407–419.
- (19) Matteson, D. S.; Majumdar, D. Homologation of boronic esters to α -chloro boronic esters. *Organometallics* **1983**, *2*, 1529–1535.
- (20) (a) Matteson, D. S.; Sadhu, K. M. Synthesis of 1-amino-2-phenylethane-1-boronic acid derivatives. *Organometallics* **1984**, *3*, 614–618. (b) Jagannathan, S.; Forsyth, T. P.; Kettner, C. A. Synthesis of boronic acid analogues of α -amino acids by introducing side chains as electrophiles. *J. Org. Chem.* **2001**, *66*, 6375–6380.
- (21) Adams, J.; Behnke, M.; Chen, S.; Cruickshank, A. A.; Dick, L. R.; Grenier, L.; Klunder, J. M.; Ma, Y. T.; Plamondon, L.; Stein, R. L. Potent and selective inhibitors of the proteasome: dipeptidyl boronic acids. *Bioorg. Med. Chem. Lett.* **1998**, *8*, 333–338.
- (22) Chatterjee, S.; Iqbal, M.; Menta, E.; Oliva, A. Method for Preparing Methyl 2-Diphenylmethylsulfonylacetate. U.S. 7,233,745, 2007.
- (23) Pallombella, V. J.; Conner, E. M.; Fuseler, J. W.; Destree, A.; Davis, J. M.; Laroux, F. S.; Wolf, R. E.; Huang, J.; Brand, S.; Elliott, P. J.; Lazarus, D.; Parent, L.; Stein, R.; Adams, J.; Grisham, M. B. Role of the proteasome and NF- κ B in streptococcal cell wall-induced polyarthritis. *Proc. Natl. Acad. Sci. U.S.A.* **1998**, *95*, 15671–15676.
- (24) Teicher, B. A.; Ara, G.; Herbst, R.; Palombella, V. J.; Adams, J. The proteasome inhibitor PS-341 in cancer therapy. *Clin. Cancer Res.* **1999**, *5*, 2638–2645.
- (25) Piva, R.; Ruggeri, B.; Williams, M.; Costa, G.; Tamagno, I.; Ferrero, D.; Giaf, V.; Coscia, M.; Peola, S.; Massaia, M.; Pezzoni, G.; Allievi, C.; Pescalli, N.; Cassin, M.; Camussi, G.; Jones-Bolin, S.; Hunter, K.; Zhao, H.; Neri, A.; Palumbo, A.; Berkers, C.; Ovaa, H.; Bernareggi, A.; Inghirami, G. CEP-18770: a novel orally-active proteasome inhibitor with a tumor-selective pharmacological profile competitive with bortezomib. *Blood*, in press.

JM7010589